ELSEVIER

Chemical Geology 209 (2004) 49–65

CHEMICAL GEOLOGY
INCLUDING
ISOTOPE GEOSCIENCE

www.elsevier.com/locate/chemgeo

Ontogenetic trace element distribution in brachiopod shells: an indicator of original seawater chemistry

Xinqing Lee[a,*], Ruizhong Hu[b], Uwe Brand[c], Hui Zhou[a], Xiaoming Liu[d], Honglin Yuan[d], Chongling Yan[e], Hongguang Cheng[a]

[a] *State Key Laboratory of Environmental Geochemistry, Institute of Geochemistry, Chinese Academy of Sciences, Guiyang GUIZHOU 550002, China*

[b] *Laboratory of Ore Deposit Geochemistry, Institute of Geochemistry, Chinese Academy of Sciences, Guiyang 550002, China*

[c] *Department of Earth Sciences, Brock University, St. Catharines, Ontario, Canada L2S 3A1*

[d] *Key Laboratory of Continental Dynamics, Department of Geology, Northwest University, Xi'an 710069, China*

[e] *School of Life Sciences, Xiamen University, Xiamen 361005, China*

Received 26 March 2003; accepted 13 April 2004

Abstract

Articulated fossil brachiopod shells have been used extensively to extract primary chemical information of Phanerozoic seawater. Despite the selection of well-preserved shells using trace element, microstructure and cathodoluminescence criteria, there are still concerns as to whether the selected brachiopod shells do indeed contain original seawater signals. Analyzed in-situ by Laser Ablation-Inductively Coupled Plasma-Mass Spectrometry (LAICPMS), Sr, Na, Mg, Mn, B and Ba distribute symmetrically in shell transects of the modern brachiopods *Magellania flavescens* and *Terebratulina septentrionalis*. Symmetry of the trace element distribution pattern is considered an intrinsic and original ontogenetic property of the brachiopod shell chemistry. The trace element distribution is symmetrical in a well-preserved shell of the Devonian brachiopod *Independatrypa lemma*, indicating that the selected shell by the conventional criteria has preserved its original seawater signal for 400 Ma. In another specimen of *I. lemma* that is considered diagenetically altered, trace element concentrations are asymmetrically distributed in the shell. The agreement between the distribution criteria and the conventional methods indicates the latter can be used to select brachiopod shells with original seawater chemistry. The average element concentration in the whole shell of unaltered brachiopods should be a reflection of the seawater chemistry, while its change in different part of a shell reflects ontogenetic effect, and its high frequent fluctuations in a transect are results of changes in environmental parameters with seasonal or annual characteristics.

Keywords: Brachiopod; Trace element; Symmetric ontogenetic distribution; Laser ablation ICP mass spectrometry; Original seawater indicator; Biogeochemistry

1. Introduction

Articulate brachiopod shells have been used extensively for studies of secular trends in $\delta^{18}O$, $\delta^{13}C$ and Sr^{87}/Sr^{86} of Phanerozoic seawater (e.g., Veizer and

* Corresponding author. Tel.: +86-851-589-1611; fax: +86-851-589-1611.

E-mail address: xinqinglee@hotmail.com (X. Lee).

0009-2541/$ - see front matter © 2004 Elsevier B.V. All rights reserved.
doi:10.1016/j.chemgeo.2004.04.029

Hoefs, 1976; Burke et al., 1982; Popp et al., 1986; Veizer et al., 1986; Brand, 1989b; Wadleigh and Veizer, 1992; Qing and Veizer, 1994; Diener et al., 1996; Veizer et al., 1997a; Veizer et al., 1997b; Qing et al., 1998; Azmy et al., 1999), of thermohaline circulation in ancient oceans (Railsback et al., 1989; Railsback, 1990; Zachos et al., 1993), as well as for studies of paleoenvironment and paleoclimate (e.g., Brand, 1989a; Grossman et al., 1991; Bates and Brand, 1991; Lavoie, 1993; Grossman et al., 1993; Talent et al., 1993; Wenzel and Joachimski, 1996; Bruckschen and Veizer, 1997; Bickert et al., 1997; Mii et al., 1997; Azmy et al., 1998; Mii et al., 1999). Brachiopods secrete a low-Mg calcite shell generally in oxygen isotopic equilibrium with ambient seawater, and which is relatively resistant to diagenetic alternation (Lowenstam, 1961; Carpenter and Lohmann, 1995; James et al., 1997; Brand et al., 2003). In order to identify shells as suitable proxies for original seawater signals, they have to be evaluated by a number of criteria such as trace elements, microstructures and cathodoluminescence (CL). As a general rule, shells with high Sr and Na and low Fe and Mn contents comparable to modern brachiopods, plus retentive textures as well as nonluminescence are considered well-preserved. Brachiopods with high Fe and Mn and low Sr and Na contents, or fabric-dissolved microstructures, or strong luminescence are considered diagenetically altered (e.g., Brand and Veizer, 1980; Veizer, 1983a,b; Popp et al., 1986; Grossman et al., 1993; Grossman et al., 1996; Bickert et al., 1997; Veizer et al., 1997a; Qing et al., 1998; Mii et al., 1999). Questions, however, linger about the veracity of these tests and thus the reliability of fossil brachiopod shells as proxies of original seawater chemistry (Rush and Chafetz, 1990; Banner and Kaufman, 1994; Land, 1995). This is particularly true for elemental/isotopic analyses of brachiopods older than Mid-Ordovician (Land, 1995; Veizer, 1995).

Conventional selection criteria are relative standards in distinguishing well-preserved shells from diagenetically altered ones. However, it seldom addresses the question as to whether the well-preserved specimen also preserves original seawater chemistry, which is usually considered a de facto conclusion. The key is to find some incontrovertible test that unequivocally identifies the original chemical state of the brachiopod low-Mg calcite shell. This would clarify the crucial issue as to whether fossil shells may indeed preserve original-seawater chemistry signals. In this study, we propose a new process and procedure to assess the shell's original state by evaluating the symmetry of the element distribution in transverse section. Specifically, this process relies on a thorough and in-situ analysis of modern and fossil brachiopod shells by Laser Ablation-Inductively Coupled Plasma-Mass Spectrometry (LAICPMS). Identification of unaltered shells with original chemistry relies on symmetric ontogenetic trace-element distribution in transverse section, and thus determines the brachiopod specimens which may serve as proxies of original seawater chemistry.

2. Study material

The modern brachiopods are *Magellania flavescens* and *Terebratulina septentrionalis* (hereafter referred to as *Mag* and *Tereb*, respectively), which are from Westerport Bay, Victoria, Australia, and the Bay of Fundy, Canada, respectively (Brand et al., 2003). The pedicle valve of *Mag* is about 3 cm long and 2 cm wide with a shell thickness of about 2 mm, whereas that of *Tereb* is 1.6 cm long, 1.4 cm wide and about 1 mm thick. In cross-section both shells exhibit the fibrous calcite layer, which is approximately parallel to the shell surface and with micro-pores transecting the fibers (Fig. 1A,B). Despite the punctuate nature of the shells, the modern brachiopods are deemed free of any signs of diagenesis (Brand et al., 2003).

The two fossil brachiopods analyzed are *Independatrypa lemma* (hereafter referred to as IL-1 and IL-2) and were collected at Guixi in the fore-belt of the Longmenshan Mountains, China (for geological background, see Lee and Wan, 2000). The fossil specimens are from strata represented by the benthic community *Independatrypa lemma–Uncinulus heterocostellis–Emanuella takwanensis* (Chen and Wang, 1996). The sediments were deposited in a lagoon on the leeward side of a barrier coral reef associated with a gradual sea level drop (Liu et al., 1996) during the Givetian (Middle Devonian).

The fossils are similar in size; about 4 cm long and 3 cm wide (Fig. 1C,D). Maximum thickness of 9 mm of the pedicle valve is attained in the umbo area. In cross-section, the shells reveal two textural components: a fibrous calcite layer and an underlying (inner)

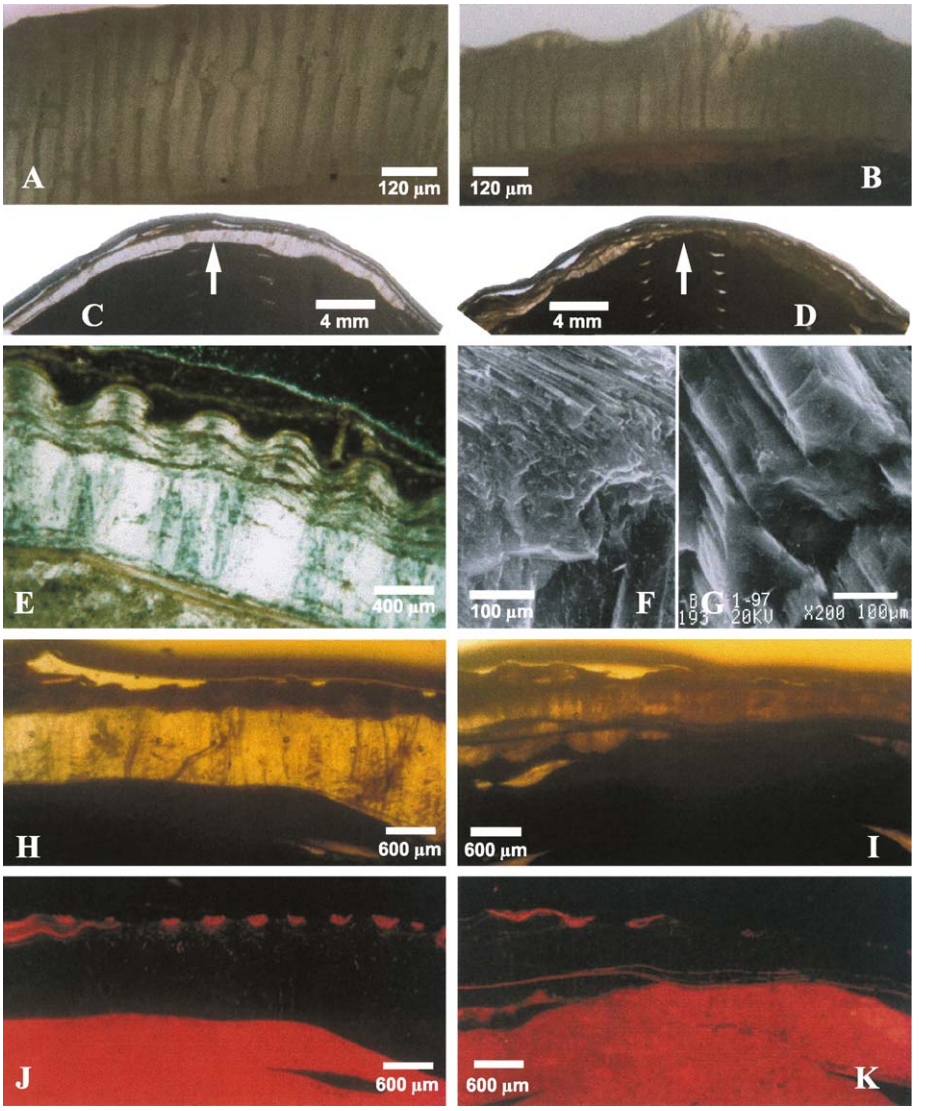

Fig. 1. Microphotograph of shell structure in modern brachiopods *M. flavescens* (A, × 80) and *T. septentrionalis* (B, × 80); shell transects of mid Devonian *I. lemma* (IL-1 ,C, × 3 and IL-2, D, × 3). The arrows in pictures C and D indicate where the symmetry line of prismatic layer crosses the transects; shell structure of the fossil *I. lemma* (E, × 20). The upper part of picture E is the fibrous layer, the light band with darker streaks is the prismatic layer. SEM image of *I. lemma* with fibrous crystals (F, × 200) and crystals in the prismatic layer (G, × 200). Microphotograph of central segment of shell under plane polarized light (IL-1, H, × 15; and IL-2, I, × 15), and corresponding views under CL (J, × 15 and K, × 15). Operating condition for cathode luminescence is 0.5 mA current, 10 kV voltage and 22 min for film exposure. The small dots in the prismatic layer in H and I represent analytical points. Prismatic calcite in both IL-1 and IL-2 does not luminesce, while the fibrous layer and limestone are brightly luminescent.

prismatic layer (Fig. 1E,F). Thickness of the fibrous layer is relatively uniform throughout the whole shell, while the prismatic layer is roughly symmetrical in transverse section (Fig. 1C,D). As a result, the symmetrical plane based on morphological observation may not necessarily coincide with that of the prismatic layer.

The calcite crystals in the prismatic layer of the two shells are tightly packed without any signs of dissolution (SEM; Fig. 1G). Under microscope, however, prismatic

layer of IL-1 is much clearer than that of IL-2, which has more secondary 'streaks' (Fig. 1C,D,H,I). Corresponding with microscopic features, IL-2 has more yellow-red streaks than IL-1 in CL (Fig. 1J,K). Therefore, by conventional selection criteria, the shell of IL-1 is deemed well-preserved, while that of IL-2 is deemed less well-preserved or diagenetically altered.

3. Analytical techniques

3.1. Instrument

The experiments were carried out in the LAICPMS laboratory of Northwest University, Xi'an. The ICP-MS used is an Elan 6100 DRC (Dynamic Reaction Cell). The instrument has a sensitivity of about 90 million counts per second (cps) for 1 μg ml[i©1] of ln when operated in the standard-solution nebulisation mode (Meinhard concentric nebulizer and cyclonic spray chamber). Background intensities are usually a few cps for elements above m/z = 85 (Rb), except for Sn and Pb, which might reach 100–200 cps due to memory effects.

The GeoLas 200 M laser-ablation system (MicroLas, Göttingen, Germany) was used for the laser ablation experiments. The system is equipped with a 193 nm ArF-excimer laser and a homogenizing, imaging optical system. The set-up delivers a flat top beam onto the sample surface and the laser wavelength and energy density (40 J·cm^{-2}) allows the controlled ablation of highly transparent samples (Gunther et al., 1997). The spot size can be varied from between 4 and 120 μm by means of an aperture system, which provides a constant energy density at the ablation site for variable spot sizes. A spot size of 60 μm was used throughout this study. Helium was used as the carrier gas to enhance transport efficiency of ablated material. The helium carrier inside the ablation cell was mixed with argon before entering the ICP to maintain stable and optimum excitation conditions. The operating parameters of the instruments are summarized in Table 1.

Table 1
Instrumental parameters

ELAN 6100 DRC ICP-MS	
Nebulizer gas flow	0.60–0.80 l·min^{-1}
Auxiliary gas flow	0.60–0.90 l·min^{-1}
Plasma gas flow	11–15 l·min^{-1}
Lens voltage	3.5–10 V
ICP RF power	1050–1350 W
Auto lens	On
GeoLas laser ablation system	
He carrier gas flow	0.67 l·min^{-1}
Energy (10 Hz)	168–210 mJ
Spot size	60 μm
Laser frequency	10 Hz

3.2. Data acquisition and reduction

All measurements were carried out using time-resolved analysis operating in fast, peak jumping mode (one point per mass peak, 10 ms of dwell time per isotope and a quadruple settling time of 2 ms, one sweep per reading and 200 readings for one replicate). Each spot analysis consisted of approximately 30 s background acquisition (gas blank) followed by 60 s data acquisition from the sample. Seven isotopes (^{42}Ca, ^{11}B, ^{23}Na, ^{25}Mg, ^{55}Mn, ^{88}Sr, ^{137}Ba) were measured with each isotope's total integration time of 1.2 s. Gas blank was typically 1000–2000 cps for Ca and Mn; 100–500 cps for Na; and <10 cps for Mg, Sr (Gao et al., 2002).

3.3. Quantification

Instruments were calibrated with multi-element glass standard NIST-SRM 610 (US National Institute of Standard and Technology—Standard Reference Material) in conjunction with internal standardization using Ca (Longerich et al., 1996; Gunther et al., 1999). Elemental concentrations of NIST SRM 610 used for external calibration are from Pearce et al., 1997. Internal standardization was used to correct for differences in ablation yield between samples and reference material. Additionally, internal standardization also partially corrected for matrix effects and signal drift of the ICP-MS (Longerich et al., 1996; Gunther et al., 1999).

Signal intensities (count rate) were recorded for the isotope of the analytes. The concentration of an element in the sample ($C_{AN_{SAM}}$) is given by the count rate for the analyte ($R_{AN_{SAM}}$) in the sample divided by the normalized sensitivity (S):

$$C_{AN_{SAM}} = R_{AN_{SAM}}/S$$

$$S = \frac{R_{AN_{CAL}}}{C_{AN_{CAL}}}\left(\frac{R_{IS_{SAM}}}{R_{IS_{CAL}}}\frac{C_{IS_{CAL}}}{C_{IS_{SAM}}}\right)$$

where $R_{AN_{CAL}}$ is the count rate of the analyte in the calibration material; $C_{AN_{CAL}}$ is the concentration of the analyte element in the calibration material; $R_{IS_{SAM}}$ is the count rate of the internal standard in the sample; $R_{IS_{CAL}}$ is the count rate of the internal standard in the calibration material; $C_{IS_{SAM}}$ is the concentration of the internal standard in the sample; and $C_{IS_{CAL}}$ is the concentration of the internal standard in the calibration material (Longerich et al., 1996). Calculations were carried out with the Glitter program. The element concentration is reported in ppm together with 1σ standard deviation for all specimens (Appendix A).

3.4. Shell analysis

Sections about 1 mm thick were cut perpendicular to the direction of shell growth as indicated on the figure (Fig. 2). Each section was then polished. The shell of *Mag* was analyzed with a spot interval of about 0.3 mm LAICPMS, while the other specimens were analyzed with spot intervals of about 0.5 mm (see Appendix A for precise interval parameters). Given the thickness heterogeneity of the prismatic layer of *I. lemma*, all analytical points were aligned as much as possible the same distance from the periphery of the prismatic layer.

The average relative standard deviations (RSD) for the analyses of *Mag* and *Tereb* are shown in Table 2. Since the modern shells are unaltered, their RSDs can be regarded as values representing analytical uncertainty. Given the heterogeneity of the shell composition, the true uncertainty of the analyses may be lower than the presented values. The average RSD of the trace elements Sr, Na, Mg and even Mn is between 3% and 7%, matching the uncertainty of $<10\%$ obtained with standard reference material (Gao et al., 2002). In contrast, the RSD for Ba is high with 15%, and for B it is 30%, these high errors are partly due to their low concentrations. Therefore, the concentrations for Ba and B are deemed less reliable 'preservation indicators' than Sr, Na, Mg and Mn. Despite the high degree of uncertainty for Ba and B, all analytical results may be used as primary and secondary indicators of original shell chemistry preservation (Appendix A).

Table 2
Average RSD (%) for the analysis of modern brachiopods (*M. flavescens* [*Mag*] and *T. septentrionalis* [*Tereb*])

Element	*Mag*	*Tereb*
Sr	5.4	3.2
Na	5.6	3.6
Mg	6.0	5.8
Mn	11.8	6.6
Ba	14.3	16.2
B	29.7	21.8

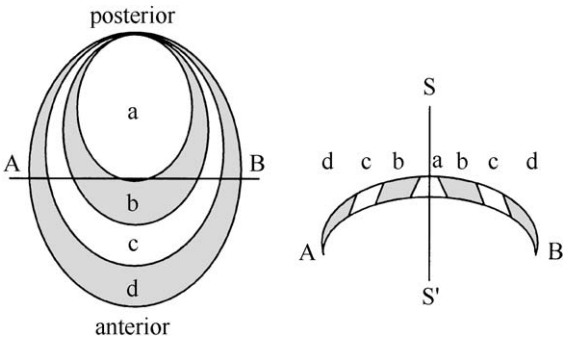

Fig. 2. Schematic showing growth bands of brachiopod shell (the left graph, top view) and the band distribution in transverse section along line A–B (the right graph). Distribution of growth band is symmetrical about a line through the middle of the transect (symmetry line of the bands shown as S–S′; letters a, b, c, and d denote growth bands).

4. Results and discussion

Shells of articulated brachiopods are secreted at the margin by its outer epithelium of the mantle. Shell growth consists of a process of circumferential enlargement (Rudwick, 1959), and the growth bands are characterized by concentric ornamental lines on the shell surface (Fig. 2). Growth is three-dimensional although the growth rate in the three directions may be different. Circumferential growth is faster than the shell's thickening process (see Williams, 1966; Williams, 1968 for detail). As a result, newly developed shell units are oriented not parallel to the shell's surface but rather across it in a specific angle (Fig. 2).

During shell growth, brachiopods incorporate trace elements into the shell's mineral lattice, a process dependent on crystal chemistry of the shell mineralogy, physiology of the organism, and physicochemical conditions of the ambient sea water (Lowenstam, 1961; Dodd, 1967; Morrison and Brand, 1986; Buening and

Carlson, 1992; Grossman et al., 1996; Rao, 1996; Lea et al., 2000). Therefore, growth band formation results in distribution of the trace element concentration, which, if not subjected to diagenetic alternation, should distribute symmetrically in bilateral section (Fig. 2).

It is noteworthy, however, that the direction of the section influences the appearance of the band distribution in the transverse thus that of trace elements. If the sections A–B in Fig. 2 is cut non-perpendicular to the direction of posterior–anterior, with the side A slightly forward to anterior while the B backward to posterior, for example, then the growth band a and b would be wider in the right side to the symmetry line, while c and d would be wider in the opposite side. The bias of the band width in the section would certainly lead to bias of distribution pattern of trace elements.

4.1. Element distribution in M. flavescens

A total of 56 points were analyzed for Sr, Na, Mg, Mn, Ba and B along the transverse section of a shell of *Mag* (Fig. 3). Strontium concentration, in general, is low in the centre (around the symmetry line) of the shell transect and then increases laterally, on both sides, to high values around 3 and 17 mm, respectively (Fig. 3A). After the high values, the element decreases bilaterally. Sixth-degree regression and statistical analysis highlight the documented chemical trends, which describe an upside-down-W pattern

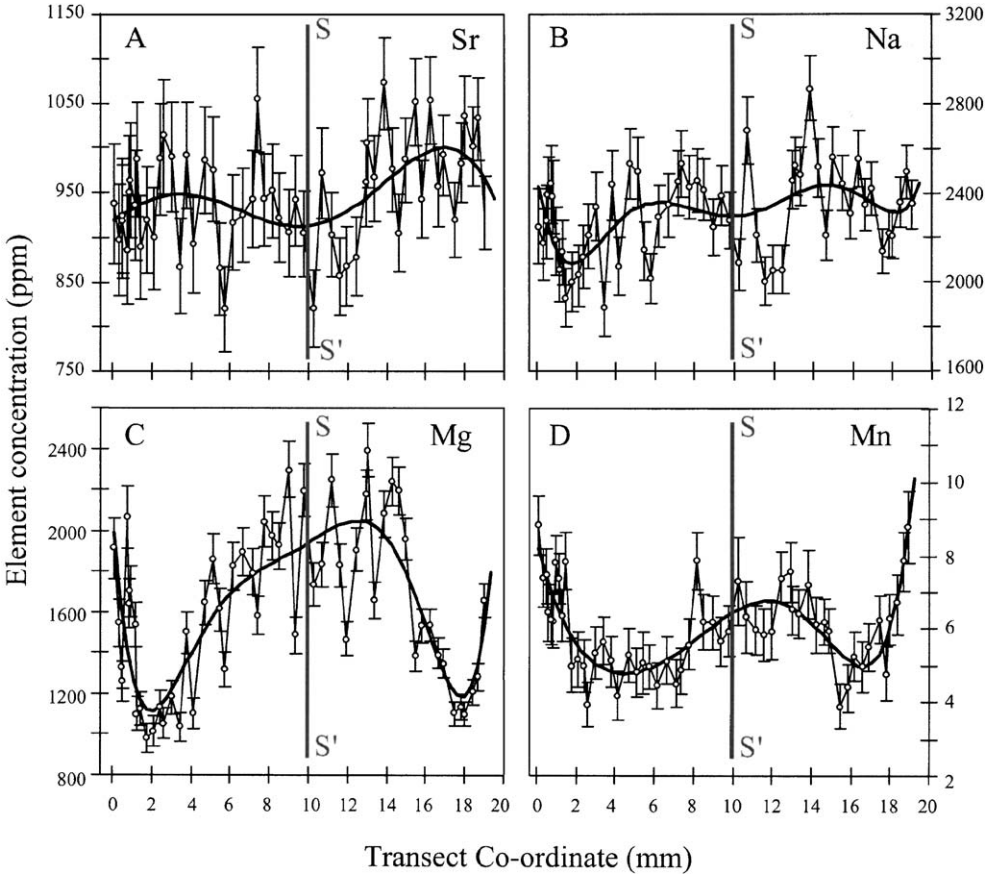

Fig. 3. Trace element distribution in transverse section of modern brachiopod *Magellania flavescens*. The individual diagrams show the chemical trends for Sr (A), Na (B), Mg (C) and Mn (D) along the shell transect. The error bar represents 1σ standard deviation and the sinusoidal line represents the sixth-order regression line. The straight line S–S′ represents the symmetrical line for the prismatic layer. The same with the following figures.

(Fig. 3A). They reveal that Sr distribution is symmetric about the symmetry line reflecting ontogenetic variation of brachiopod chemistry. No significant difference was noted between the ontogenetic bilateral-transects for Sr and the other elements (Table 3). Na also reveals a low concentration around the symmetrical line in comparison with the two shoulders around 5 and 15 mm, respectively. Furthermore, the element shows another bilaterally symmetrical cycle, it decreases and then increases following the initial chemical highs on the shoulders thus forming a stylized 'double-W' pattern to the whole transect (Fig. 3B).

In contrast to Sr and Na, the chemical concentrations for Mg and Mn follow different patterns along the shell transect (Fig. 3C,D). They start off with a high concentration in the center, and this is followed by a bilateral decrease in chemical concentrations and an inflection of increases toward the shell edge; thus forming the shape of a ''W''. The ontogenetic symmetry of Mg and Mn is more pronounced than that of Sr and Na (Fig. 3), which is accentuated by the p values of the statistical analysis. These are 0.060 and 0.058 for Sr and Na, respectively, and are 0.229 and 0.336 for Mg and Mn, respectively (Table 3). Of special interest is the high frequent fluctuations of the elements, or the small 'V' shape of the chemical compositions within a few mm (Fig. 3). These detailed trends support the assertion of not only an ontogenetic origin for the shell chemistry but more importantly it reflects the original physico-chemistry of the ambient seawater.

Table 3
ANOVA statistical analysis of bilateral (Right—R and Left—L) chemical shell-transects of *Magellania flavescens* (*Mag*) and *Terebratulina septentrionalis* (*Tereb*)

Element (ppm)	*N*	Mean	SD	*p*
M. flavescens				
Sr–R	24	960	66	
Sr–L	32	930	51	0.060
Na–R	24	2355	215	
Na–L	32	2253	182	0.058
Mg–R	24	1682	400	
Mg–L	32	1556	379	0.229
Mn–R	24	6.2	1.1	
Mn–L	32	5.9	1.2	0.336
T. septentrionalis				
Sr–R	11	1158	54	
Sr–L	12	1130	61	0.254
Na–R	11	2900	222	
Na–L	12	2860	224	0.668
Mg–R	11	2157	345	
Mg–L	12	2064	384	0.542
Mn–R	11	24.5	3.3	
Mn–L	12	24.7	3.9	0.933

The confidence interval is set at 95% ($p = 0.05$).

Despite the attention that has been put to the perpendicularity of the transect in cutting and polishing the thin slice. The transect of *Mag* was not cut exactly perpendicular to the symmetrical plane of the prismatic layer, but with left side forward and the right side backward slightly (refer to Fig. 2). As a result, to element Mg and Mn that are generally high in the shell's central part like band a and b in Fig. 2, the nonperpendicularity leads to the shift of statistical high values to the right side. Meanwhile, the low value band like band c in Fig. 2 has more portion in the left side of the transect, thus resulting in the relatively wider valleys. The nonperpendicularity disturbed the perfectness of the symmetrical distribution in the whole transect.

4.2. Element distribution in T. septentrionalis

A total of 23 points were chemically analyzed along the shell transect of *Tereb*. Sr and Na concentrations exhibit similar distribution patterns that are low around the symmetry lines in the middle followed by bilateral sinusoidal trends (Fig. 4A,B). The trends of Sr and Na in *Tereb* resemble that depicted by Na in a shell transect of *Mag*. (Fig. 3B). In contrast to the former elements, Mg and Mn have high concentrations around the symmetry lines and decrease bilaterally producing a symmetrical distribution describing a flattened omega (Ω) symbol (Fig. 4C,D). Statistical analysis supports the bilateral distribution trends for Sr, Na, Mg and Mn in *Tereb* (Table 3). The results strongly confirm the chemical symmetry about the line of symmetry for this modern brachiopod.

Although the distribution patterns and ultimate concentrations (means and ranges, Table 4) of the elements in the two modern brachiopods are not necessarily the same, they share one important characteristic, which is the ontogenetic symmetric distribution patterns. The symmetry of elements in the shell transects of the modern brachiopods *Mag* and *Tereb* testifies to their primary and original nature of the distributions and compositions. Thus ontogenetic symmetric chemical distribution patterns in brachiopods may not only identify well-preserved specimens,

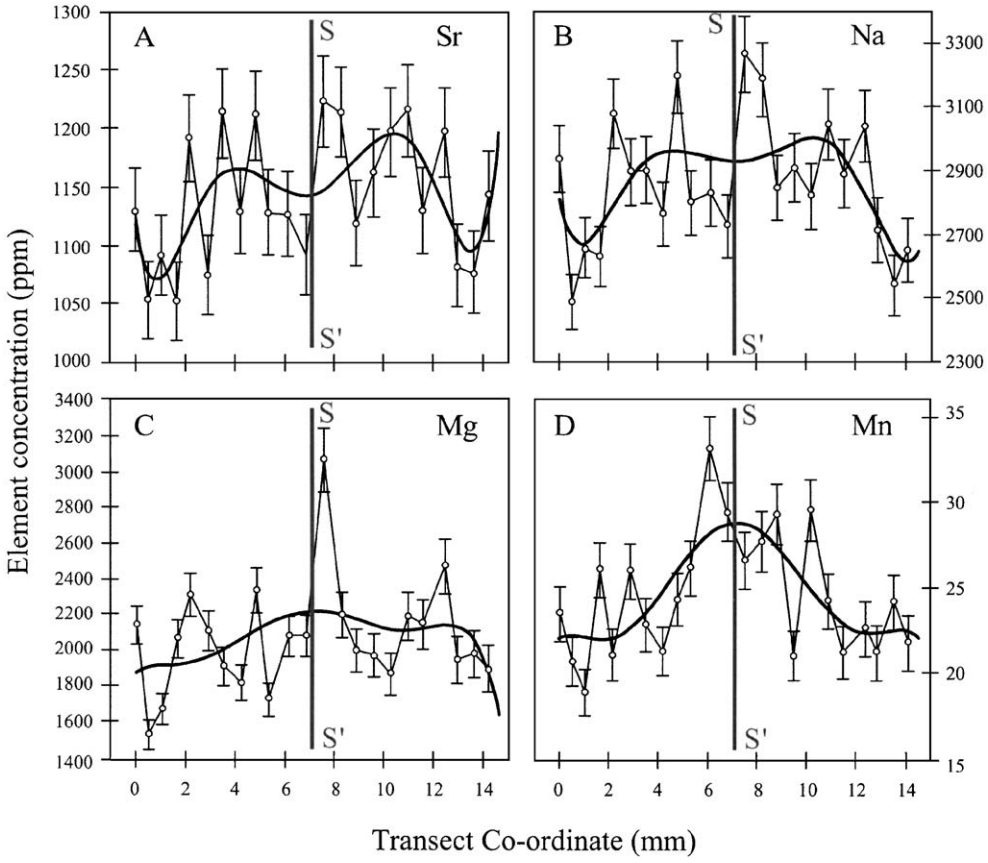

Fig. 4. Trace element distribution in transverse section of modern brachiopod *Terebratulina septentrionalis.* The individual diagrams show the chemical trends for Sr (A), Na (B), Mg (C) and Mn (D) along the shell transect. The error bar represents 1σ standard deviation and the sinusoidal line represents the sixth-order regression line.

but more importantly may identify those that have retained primary chemistry. Thus the symmetric ontogenetic trace-element distribution suggests that brachiopods which exhibit these patterns may unequivocally serve as proxies/indicators of original ambient seawater chemistry.

4.3. Shell diagenesis

If a shell is altered by diagenesis, the symmetric distribution may inevitably be changed. Weak textual portions such as alveolae, or intercrystal boundaries originally formed during shell growth, and

Table 4
Means and ranges of trace elements (LAICPMS) in shell transects *of Magellania flavescens* (*Mag*) and *Terebratulina septentrionalis* (*Tereb*), as well as of the Devonian brachiopod *Independatrypa lemma* (IL-1 and IL-2)

Element (ppm)	*Mag*	*Tereb*	IL-1	IL-2
Sr	946, 820–1072	1141, 1052–1222	526, 353–958	427, 367–586
Na	2300, 1879–2867	2863, 2486–3270	232, 75–836	158, 59–951
Mg	1608, 978–2391	2066, 1531–3059	1924, 411–5973	587, 253–3892
Mn	6.0, 3.9–8.8	24.5, 18.9–33.2	14.6, 2.0–87.0	5.8, 3.7–16.6
Ba	2.0, 1.5–2.7	2.4, 1.6–3.1	0.8, 0.2–2.3	0.6, 0.0–7.7
B	39.0, 22.7–58.4	70.4, 41.3–91.0	9.2, 4.3–34.6	8.6, 6.3–25.5

secondary fractures in lines or bands that formed under post-depositional stresses (e.g., Popp et al., 1986; Grossman et al., 1991; Veizer et al., 1997a; Lee et al., 1999), are susceptible to permeation of diagenetic fluid(s). Diagenetic alternation, therefore, may change the shell preferentially along weak structures/features thus disturbing the element distribution pattern and concentrations. If trace elements in transects distribute evenly, it does not suggest changes of element during formation of the shell but rather a homogeneous post-depositional alternation effect. Therefore, whether or not trace elements distribute symmetrically in transverse sections of a brachiopod shell may be used to infer the shell's degree of preservation.

4.4. Element distribution in I. lemma (IL-1 and IL-2)

Two Givetian brachiopod specimens of *I. lemma* were analyzed by LAICPMS to determine their preservational status and potential for retaining original seawater chemistry. A total of 42 and 41 points were analyzed for trace elements along the shell transects of specimens IL-1 and IL-2, respectively. Sr, Na, Mg and Mn in IL-1 have high concentrations in the middle part (also around the symmetry line) of the shell transect and then laterally show a decrease followed by an increase towards the edges. Consequently, all elements distribute in a "W" shape pattern (Fig. 5A–D). This symmetrical elemental distribution indicates that specimen IL-1 is not only well-preserved, but more

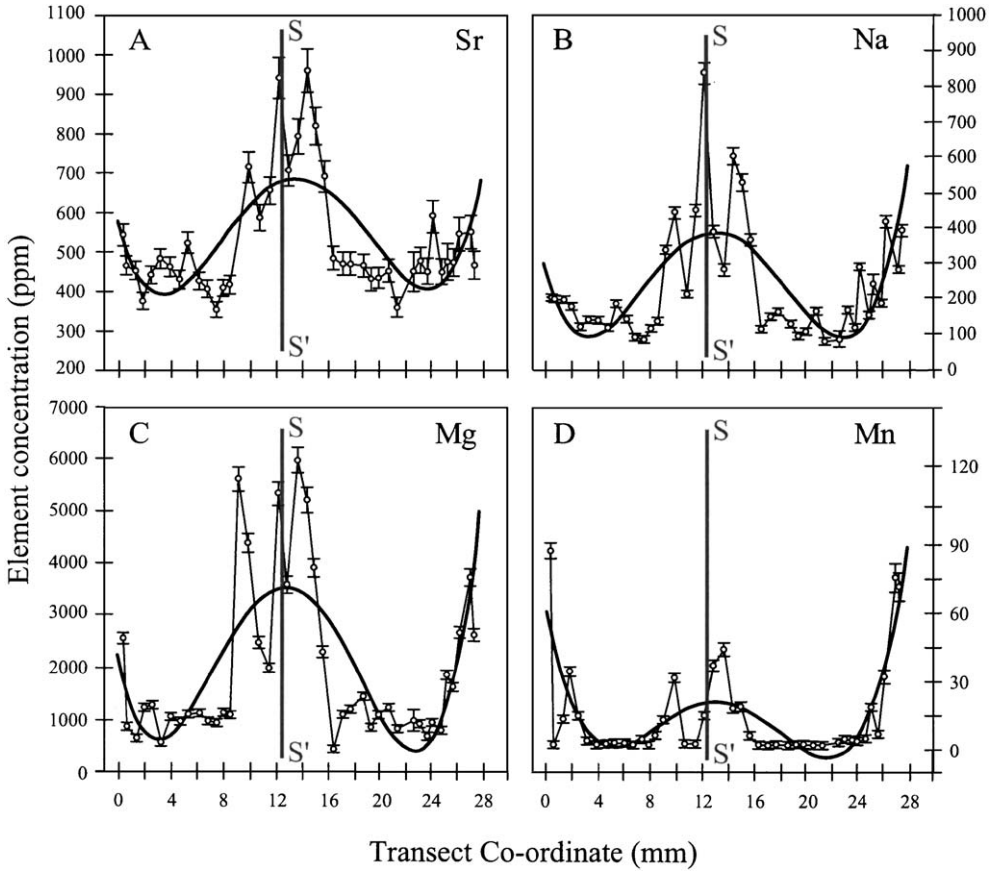

Fig. 5. Trace element distribution in transverse section of Devonian *Independatrypa lemma* (IL-1). The individual diagrams show the chemical trends for Sr (A), Na (B), Mg (C) and Mn (D) along the shell transect. The error bar represents 1σ standard deviation and the sinusoidal line represents the sixth-order regression line.

importantly its shell chemistry is a reflection of the original ambient seawater.

Quite different to the distribution of their counterparts in IL-1, none of the elements in IL-2 exhibit symmetrical distribution (Fig. 6A–D). Not only are IL-2 and IL-1 the same species, but also from the same stratum. Consequently, they must have experienced the same living conditions, and thus exhibited similar elemental distribution patterns if both are equally well preserved, Since this is not the case, it is assumed that specimen IL-2 was subjected to some degree of post-depositional alteration. The preservation interpretations for these two Devonian specimens are in line with the results of conventional evaluation criteria, namely specimen IL-1 is well preserved, whereas specimen IL-2 is diagenetically altered (in part Table 4). Nevertheless, specimen IL-1 is well preserved, it may serve as a proxy/indicator of original seawater chemistry during its lifespan.

4.5. Elemental comparison between modern and fossil brachiopods

Trace chemistry of brachiopods, modern and fossil might achieve a degree of covariance. However, simple transposition of modern brachiopod chemistry to fossil counterparts should be considered in light of evolutionary changes on the biogeochemistry of the fossil brachiopods, as well as on the chemistry of the ocean. Comparison of *I. lemma* trace chemistry with that of the two modern specimens leaves a lot of room for speculation (Table 4). It may be misleading to judge a fossil shell's preservation state simply by the trace element concentration criterion. As shown in Table 4,

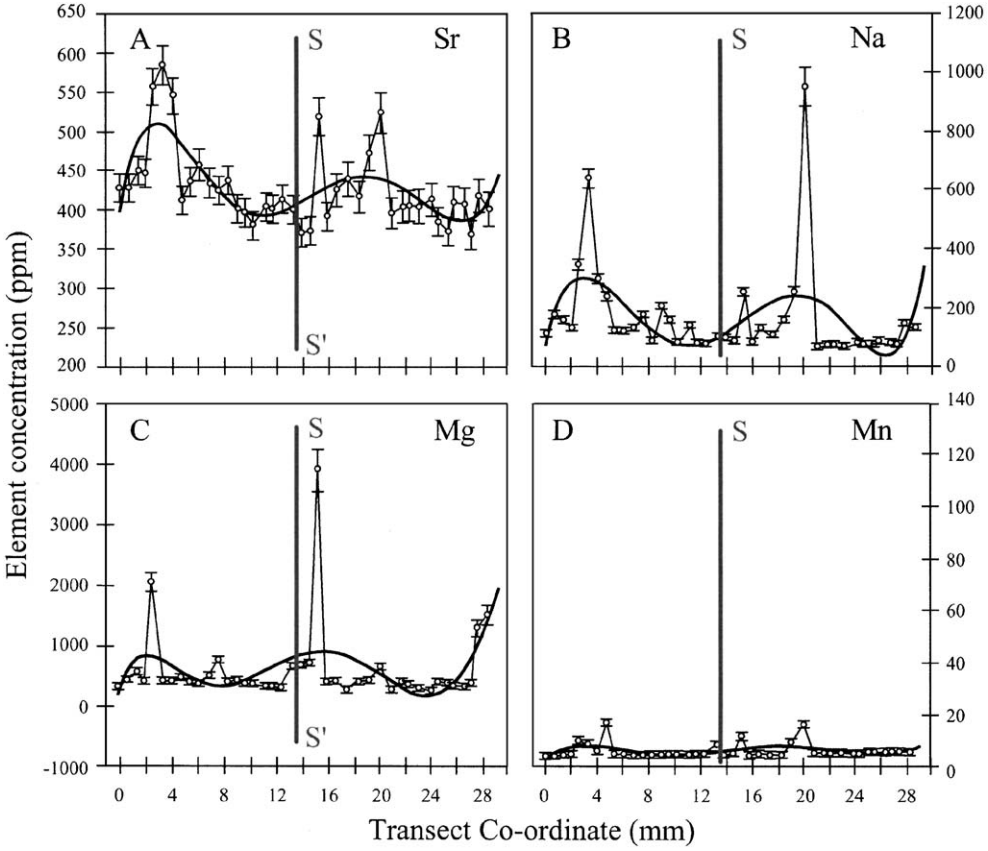

FIg. 6. Trace element distribution in transverse section of Devonian *Independatrypa lemma* (IL-2). The individual diagrams show the chemical trends for Sr (A), Na (B), Mg (C) and Mn (D) along the shell transect. The error bar represents 1σ standard deviation and the sinusoidal line represents the sixth-order regression line.

Sr and Na in IL-1 are much lower than those in *Mag* and *Tereb* although Mg and Mn are between those of *Mag* and *Tereb*. Therefore, the well preserved fossil shell may not necessarily match its modern counterpart in element concentration. Similarly, luminescence as a reliable diagenetic indicator is also questioned by the Mn chemistry obtained for specimen IL-2, where the values range from 3.7 to 16.55 ppm, most of which is below the concentration of IL-1 and even much lower than the critical value of 80 ppm generally considered necessary for luminescence (Pierson, 1981). Therefore, the shell, though generally considered diagenetically altered, is non-luminescent except for in areas of secondary calcite-filled fractures (Fig. 1; cf. Rush and Chafetz, 1990). Nevertheless, the agreement between the evaluation of the fossils by the element distribution and that by the conventional criteria suggests that the combination of trace elements, microstructures and CL is applicable for selection of shells with original seawater chemistry.

Chemistry of the seawater has long been found to be a main factor that controls the elemental chemistry in brachiopod shells (Lowenstam, 1961; Dodd, 1967), based on which, researches have been done to infer seawater chemistry from the shell measurements (e.g., Brand, 1989c; Rao, 1996). Accordingly, the average concentration of trace elements in the whole transect of *Mag*, *Tereb* and IL-1, to the first approximation, should be a reflection of the seawater chemistry. The modern brachiopods are much higher than IL-1 in Sr and Na concentration, suggesting that modern oceans may be higher in the elements than the Devonian one, given that the evolutionary effect on the element concentration is not so high. Whereas the average Mg, Mn and Ba are somewhat matchable, the Devonian ocean may be similar to the modern oceans in the element concentration.

Other parameters, such as ontogenetic variations in growth rate (Moberly, 1968; Rosenberg and Hughes, 1989; Buening and Carlson, 1992), temperature (Lowenstam, 1961; Rao, 1996; Grossman et al., 1996; Lea et al., 2000), taxonomic variations (Lowenstam, 1961; Dodd, 1967; Buening and Carlson, 1992; Grossman et al., 1996) and even fluctuations in nutrient levels (Moberly, 1968), also exert influences on incorporation of trace elements into the shell. The modern brachiopod *Mag* and *Tereb* exhibit lower Sr and Na but higher Mg and Mn in the central part (secreted during the early stage of the shell development) than in the adjacent lateral parts (secreted during the later stage of the shell development) of the transections. The variation can be as high as 1600 ppm for Mg in *Mag*. No changes in seawater chemistry can result in such a large variation within a brachiopod's lifespan. This kind of variation of the elements should be attributed to ontogenetic effect, i.e. the discrimination against the element in different stages of the shell development. It is interesting to note that both Sr and Na are higher in the central part in IL-1 (Fig. 5A,B), which is contrary to those in the modern brachiopod (Figs. 3A,B and 4A,B). Moreover, the difference of the element concentration between the central part and the adjacent lateral ones is much larger in IL-1 than in the modern species. Whether these are a reflection of evolution of the ontogenetic effect should be confirmed by more comparative studies between fossil and modern brachiopods.

The element fluctuations in the higher spatial (thus also temporal) resolution in both modern and fossil brachiopods may be the result of changes in parameters such as temperature or nutrient level, which is of annual or seasonal characters. Simple tally of the up-and-downs of the element concentration on either side of the symmetry line agrees with the speculation of longevity of brachiopods, which is from a few years to as long as two decades (Buening and Carlson, 1992; Buening and Spero, 1996), suggesting again the annual or seasonal genesis of the element fluctuations.

5. Conclusions

The modern brachiopods *M. flavescens* and *T. septentrionalis* from the southern and northern hemispheres of the globe demonstrate symmetrical trace element distribution in shell transects. It proves that symmetric trace element distribution derived from shell growth bands is an intrinsic and ontogenetic characteristic of the organism. Brachiopod shells can be examined as to their preservation state in terms of the distribution, and furthermore it indicates the high potential of symmetry studies in identifying brachiopods as indicators/proxies of original seawater chemistry.

I. lemma (IL-1), a well-preserved fossil brachiopod by the conventional criteria, exhibits a symmetric elemental pattern for all studied elements, indicating

that it does preserve its original composition in millions of years, and thus can be used to reconstruct the seawater chemistry of paleoceans. While in a diagenetically altered brachiopod, IL-2, the elements do not demonstrate symmetrical distribution. The agreement between the distribution method and the conventional criteria in evaluating preservation state of *I. lemma* suggests that the relative criteria can be used to select shells with original seawater chemistry.

The average element concentration of the whole shell of both modern and fossil brachiopods should be a reflection of the seawater chemistry. Our comparison of the modern brachiopods and the fossils suggests that modern oceans might be higher in Sr and Na concentration than the Devonian ocean, while they might be similar in Mg, Mn and Ba. The element variation from the central part to the bilateral of a shell is a result of ontogenetic effect, whereas the high frequent fluctuations of the elements are reflections of changes in environmental parameters with seasonal or annual characteristics.

Acknowledgements

The authors are indebted for financial support to the Natural Science Foundation of China (Grant No. 40273011), the Key Laboratory of Continental Dynamics at Northwest University, Xi'an, the Laboratory of Ore Deposit Geochemistry and the State Key Laboratory of Environmental Geochemistry, Institute of Geochemistry, Chinese Academy of Sciences, as well as to the Natural Science and Engineering Research Council of Canada (Grant No. A7961). Thanks are also due to Professor Yuanren Chen (Chengdu University of Technology) for his help with fossil sampling in the field, Professor Jan Veizer (University of Ottawa) for his correspondence and encouragement, Dr. Kai Hartmann (Freie Universität Berlin) for his help with conversion of analytical data, and M. Lozon (Brock University) for drafting of the figures. Dr. Horng-sheng Mii and Dr. Hairuo Qing reviewed the manuscript, their constructive criticism helped with the improvement of the paper. [**EO**]

Appendix A. Geochemical dataset of the brachiopod shells

Coordinate		Concentration (ppm)						Standard deviation (1σ)					
X	Y	Sr	Na	Mg	Mn	B	Ba	Sr	Na	Mg	Mn	B	Ba
Magellania flavescens													
18.97	−3.63	926.9	2348.6	1654.2	8.8	35.4		40.4	109.1	82.9	1.0	10.4	1.0
18.68	−4.04	1032.5	2491.2	1283.9	7.9	53.5		45.7	117.3	66.5	0.8	14.7	0.8
18.39	−4.35	1000.9	2362.5	1209.9	6.7	50.0	1.9	44.5	111.8	63.2	0.8	13.9	0.3
17.99	−4.65	1033.9	2209.0	1099.2	6.3	53.7	1.6	46.2	105.0	57.3	0.7	14.6	0.3
17.80	−5.06	983.1	2218.8	1136.0	4.8	50.2	2.1	44.2	106.1	60.0	0.7	13.8	0.3
17.50	−5.26	919.4	2138.6	1103.8	6.3	37.9	1.8	41.5	102.7	58.0	0.7	10.6	0.3
16.91	−5.67	990.6	2418.7	1349.0	5.5	45.4	1.8	45.0	116.7	70.6	0.7	12.6	0.3
16.62	−6.08	955.9	2346.9	1396.9	5.0	34.5	1.9	43.7	113.9	73.6	0.7	10.1	0.3
16.22	−6.29	1052.5	2552.7	1534.9	5.3	53.2	2.0	48.4	124.5	80.4	0.7	14.5	0.3
15.83	−6.60	942.3	2304.8	1532.6	4.4	36.8	2.0	43.6	113.1	80.7	0.6	10.4	0.3
15.43	−6.70	1050.9	2444.0	1383.1	3.9	55.3	1.8	48.9	120.6	73.4	0.6	14.9	0.3
14.94	−7.01	986.6	2561.9	1957.6	5.9	47.0	2.0	46.9	128.7	104.3	0.6	12.9	0.3
14.64	−7.22	904.9	2212.9	2192.4	6.2	30.0	2.4	43.3	111.9	117.0	0.6	8.9	0.3
14.25	−7.53	975.3	2512.9	2240.3	6.1	32.5	2.7	47.0	128.0	120.9	0.8	9.8	0.4
13.85	−7.73	1071.8	2867.0	2080.7	7.2	54.4	2.6	52.0	146.9	113.4	0.9	15.1	0.4
13.35	−7.84	965.4	2474.5	1658.0	6.4	36.5	1.8	47.2	127.6	90.7	0.7	10.3	0.3
13.06	−7.95	1004.5	2521.2	2391.3	6.5	32.1	2.7	49.5	130.9	131.0	0.7	9.4	0.4
12.96	−8.15	960.5	2459.5	2176.9	7.6	37.0		47.7	128.7	120.8	0.8	10.9	0.7
12.46	−8.16	878.8	2056.0	1904.9	7.4	23.6	2.1	43.9	108.3	106.4	0.7	7.3	0.3
11.96	−8.27	867.6	2057.1	1468.5	5.9	28.0	1.7	43.7	109.2	83.8	0.8	8.7	0.3
11.56	−8.28	856.6	2003.3	1830.7	5.9	22.7	1.9	43.5	107.0	103.9	0.7	7.1	0.3
11.16	−8.39	902.3	2211.2	2246.3	6.0	28.3	2.0	46.8	120.6	128.9	0.7	8.4	0.3
10.67	−8.50	971.3	2680.5	1834.3	6.3	46.1	1.5	50.9	147.5	108.6	1.0	14.0	0.3

Appendix A (*continued*)

Coordinate		Concentration (ppm)						Standard deviation (1σ)					
X	Y	Sr	Na	Mg	Mn	B	Ba	Sr	Na	Mg	Mn	B	Ba
Magellania flavescens													
10.27	− 8.50	820.1	2080.7	1732.4	7.3	27.5		43.3	115.6	104.8	1.2	9.7	1.0
9.77	− 8.51	904.3	2277.2	2194.6	5.9	24.7	2.2	48.0	126.9	128.9	0.7	7.9	0.3
9.37	− 8.62	941.8	2387.9	1487.1	5.7	46.7	1.8	50.4	134.1	89.0	0.7	13.3	0.3
8.97	− 8.53	905.4	2249.4	2297.1	6.2	24.6	2.2	48.8	127.3	137.0	0.7	7.8	0.3
8.46	− 8.44	921.8	2413.4	1924.0	6.2	32.6		50.1	137.6	116.2	0.8	9.8	0.4
8.16	− 8.34	952.1	2457.9	1974.4	7.9	38.5	2.0	52.1	141.1	119.9	0.8	11.5	0.3
7.76	− 8.15	942.0	2426.6	2047.0	5.6	35.3	2.4	52.0	140.4	125.0	0.7	10.5	0.3
7.36	− 8.06	1053.8	2531.5	1582.8	4.9	56.0	1.7	58.6	147.5	97.6	0.6	15.8	0.3
7.16	− 7.96	942.9	2446.8	1796.2	4.5	36.3	1.7	53.7	145.8	113.1	0.7	10.8	0.3
6.65	− 7.77	924.7	2346.1	1894.6	5.1	31.1	2.5	53.0	140.9	119.9	0.7	9.6	0.3
6.15	− 7.58	916.2	2295.4	1826.4	4.5	33.2	2.2	53.0	138.9	116.5	0.6	9.9	0.3
5.74	− 7.29	820.0	2016.5	1313.8	5.0	26.4	1.8	47.8	110.8	85.1	0.6	8.2	0.3
5.44	− 7.10	864.5	2141.3	1611.4	5.1	29.4	2.0	50.8	131.7	105.8	0.9	9.5	0.3
5.14	− 7.00	976.1	2492.2	1859.9	4.8	39.1		57.8	154.3	121.4	0.7	11.8	0.5
4.73	− 6.81	986.2	2529.9	1644.3	5.3	38.7	1.7	58.8	157.9	108.8	0.7	11.9	0.3
4.13	− 6.62	891.7	2069.9	1099.8	4.2	39.5		53.6	130.2	74.1	0.7	11.8	0.5
3.82	− 6.33	991.2	2432.8	1494.4	5.1	50.0	2.6	60.0	154.1	100.4	0.7	14.6	0.4
3.42	− 6.04	867.4	1879.2	1033.9	5.7	28.7	1.5	52.9	120.0	70.6	0.6	9.1	0.3
3.01	− 5.64	989.9	2339.1	1181.0	5.4	46.4	1.8	61.8	152.7	82.4	0.7	14.0	0.3
2.60	− 5.35	1012.7	2207.3	1051.8	3.9	58.4	2.0	63.7	145.2	73.8	0.6	17.0	0.3
2.40	− 4.95	987.1	2115.7	1131.0	5.0	52.9	2.2	62.6	140.3	80.1	0.7	15.7	0.3
2.09	− 4.46	898.8	2028.9	1014.2	5.2	36.6		57.4	135.6	72.9	0.8	11.4	0.5
1.78	− 3.97	919.2	1999.8	977.6	5.0	41.9		59.2	134.7	70.8	0.7	12.8	0.7
1.47	− 3.57	889.4	1929.4	1122.1	7.9	33.8	2.5	57.7	130.9	81.2	0.8	10.7	0.4
1.26	− 3.28	986.7	2133.1	1100.5	6.4	46.2	2.2	64.5	145.8	80.3	0.7	14.0	0.3
1.16	− 2.88	935.5	2056.2	1537.3	7.4	45.4	1.7	61.6	141.5	111.6	0.7	13.6	0.3
0.95	− 2.58	963.1	2186.6	1701.5	7.8	42.7		63.9	151.7	124.4	0.8	13.2	0.4
0.84	− 2.18	950.2	2380.4	1638.1	6.2	30.5	1.6	63.5	166.3	121.0	0.8	10.0	0.3
0.74	− 1.89	885.5	2439.3	2062.6	6.3	30.2		60.5	174.2	154.6	0.7	9.7	0.4
0.53	− 1.59	918.1	2386.9	1321.6	6.4	43.8		63.2	171.8	101.0	0.8	13.7	1.1
0.52	− 1.19	923.0	2267.8	1259.7	7.4	45.9	1.5	64.0	164.4	97.0	0.8	14.2	0.3
0.32	− 0.79	896.7	2170.4	1544.3	7.4	35.3	1.8	62.6	158.6	119.3	0.8	11.4	0.3
0.11	− 0.50	937.5	2249.6	1913.6	8.8	35.5	1.6	65.9	165.5	148.1	0.8	11.5	0.3
Terebratulina septentrionalis													
0.00	0.00	1130.2	2939.4	2142.5	23.6	67.0	3.1	35.4	103.9	106.4	1.5	13.8	0.4
0.51	− 0.28	1052.3	2486.3	1530.5	20.7	60.9	1.6	33.0	88.1	78.5	1.4	13.0	0.3
1.03	− 0.77	1091.5	2658.9	1672.5	18.9	77.8	2.3	34.2	94.2	85.8	1.3	16.0	0.4
1.64	− 1.24	1051.9	2632.2	2065.7	26.1	41.3	2.3	33.0	93.4	105.4	1.6	9.4	0.4
2.16	− 1.63	1191.1	3081.3	2309.3	21.1	81.5	3.1	37.5	109.5	119.1	1.5	17.0	0.5
2.87	− 2.00	1073.8	2897.6	2108.6	26.1	54.0	2.6	33.8	103.1	110.0	1.6	11.9	0.4
3.48	− 2.38	1212.7	2903.4	1909.8	22.9	76.1	2.5	38.2	103.5	101.6	1.6	16.1	0.4
4.19	− 2.46	1128.6	2765.3	1816.2	21.3	67.5	2.2	35.6	98.7	97.3	1.4	14.4	0.4
4.80	− 2.84	1210.7	3198.8	2335.4	24.4	85.5	2.5	38.3	114.3	125.3	1.6	17.9	0.4
5.30	− 2.92	1127.2	2800.7	1725.7	26.3	55.4	2.0	35.7	100.4	95.1	1.6	12.3	0.4
6.10	− 2.89	1125.6	2833.1	2082.9	33.2	67.4	2.4	35.7	101.9	116.4	1.9	14.6	0.4
6.81	− 2.97	1090.7	2728.1	2084.0	29.5	66.8	2.5	34.7	98.4	118.1	1.8	14.5	0.4
7.51	− 2.94	1222.3	3269.7	3059.2	26.7	82.9	2.4	39.0	118.1	173.5	1.7	17.9	0.4
8.21	− 3.02	1213.3	3186.7	2197.5	27.8	81.3	2.5	38.8	115.5	128.1	1.8	17.5	0.4
8.81	− 2.90	1117.9	2846.0	2002.8	29.3	61.5	2.4	35.8	103.4	118.7	1.8	13.7	0.4

(continued on next page)

Appendix A (*continued*)

Coordinate		Concentration (ppm)						Standard deviation (1σ)					
X	Y	Sr	Na	Mg	Mn	B	Ba	Sr	Na	Mg	Mn	B	Ba
Terebratulina septentrionalis													
9.50	−2.77	1160.8	2910.2	1972.6	21.1	78.1	2.5	37.2	106.0	118.5	1.5	16.8	0.4
10.19	−2.55	1196.7	2819.6	1869.3	29.6	78.4	2.2	38.5	103.1	114.6	1.8	17.1	0.4
10.89	−2.33	1214.7	3046.2	2190.2	24.3	91.0	2.7	39.1	111.6	135.5	1.6	19.5	0.4
11.48	−2.01	1129.3	2890.8	2147.1	21.3	51.7	2.5	36.5	106.3	135.1	1.5	12.1	0.4
12.37	−1.67	1196.2	3040.6	2468.3	22.7	89.3	2.0	38.7	112.2	157.3	1.6	19.4	0.4
12.85	−1.16	1081.6	2712.7	1949.3	21.3	63.9	2.5	35.2	100.8	129.3	1.6	14.5	0.4
13.54	−0.83	1075.9	2539.9	1980.1	24.2	64.9	2.1	35.1	94.7	132.9	1.6	14.7	0.4
14.12	−0.31	1141.1	2650.6	1898.1	21.8	74.4	1.9	37.3	99.2	130.1	1.6	16.8	0.4
Independatrypa Lemma-1													
0.40	−0.17	543.0	201.0	2546.0	87.0	8.4	2.3	28.0	7.6	98.0	3.6	4.0	0.4
0.63	−0.35	465.3	198.5	837.7	2.2	6.1	0.2	22.9	7.7	39.8	0.9	2.9	0.1
1.36	−0.80	451.4	194.1	625.6	13.4	5.2	0.6	22.3	7.6	31.8	1.3	3.0	0.2
1.91	−1.36	374.4	174.6	1210.8	34.3	7.2	0.5	18.6	6.9	54.9	2.2	4.1	0.2
2.56	−2.01	440.3	115.7	1250.3	14.9	6.9	0.4	21.9	4.9	57.7	1.5	3.8	0.2
3.21	−2.66	482.1	137.4	548.6	3.7	6.4	0.4	24.0	5.6	28.9	1.0	3.2	0.2
3.95	−3.21	461.8	135.4	1037.1	2.3	6.3	0.6	23.1	5.6	48.6	1.0	3.3	0.2
4.70	−3.76	430.4	114.0	955.4	2.6	5.3	0.3	21.7	4.8	45.7	1.0	3.2	0.1
5.33	−4.21	521.8	181.4	1086.0	3.2	8.8	0.6	26.4	7.3	51.9	1.2	3.9	0.2
6.17	−4.65	426.3	139.2	1107.1	2.9	7.6	0.4	21.7	5.7	51.6	1.0	3.7	0.2
6.81	−5.10	406.0	87.7	961.3	2.3	4.4	0.3	21.0	3.8	45.4	0.9	2.5	0.2
7.53	−5.35	353.6	81.0	929.6	4.7	4.3	0.5	18.4	3.6	44.2	1.0	2.6	0.2
8.04	−5.51	406.9	111.7	1120.2	2.1	6.0	0.6	21.3	4.6	51.7	0.9	3.1	0.2
8.54	−5.47	417.5	133.2	1088.9	6.5	6.1	0.4	22.1	5.4	50.5	1.0	3.3	0.2
9.17	−5.92	538.5	335.1	5612.3	12.9	6.4	1.0	28.7	12.6	232.5	1.2	3.1	0.2
9.99	−6.16	716.0	442.7	4370.8	31.4	13.4	1.3	38.4	16.4	182.7	2.1	4.4	0.3
10.81	−6.30	585.7	207.7	2464.0	2.6	6.3	0.4	31.8	8.1	106.2	0.9	3.2	0.1
11.61	−6.34	656.2	448.6	1975.2	2.6	13.0	0.7	35.9	16.8	87.1	0.9	4.7	0.2
12.33	−6.49	940.2	836.3	5334.9	15.0	30.9	1.8	51.9	30.6	223.6	1.3	8.1	0.3
13.03	−6.53	707.0	392.0	3579.5	36.9	11.3	1.4	39.5	14.8	153.5	2.6	4.4	0.3
13.83	−6.47	793.7	280.6	5972.5	43.9	6.6	2.3	45.3	10.9	253.4	3.0	3.6	0.4
14.53	−6.52	958.2	603.0	5209.7	18.2	34.6	1.8	55.2	22.5	222.4	1.6	9.0	0.3
15.14	−6.57	819.3	530.3	3913.6	18.7	19.4	1.2	47.8	19.9	169.1	1.6	6.1	0.3
15.84	−6.52	691.1	366.6	2283.6	6.3	17.5	0.8	40.8	13.9	101.6	1.0	5.3	0.2
16.53	−6.37	483.7	109.8	410.9	2.2	7.3	0.4	28.9	4.6	23.2	0.9	3.0	0.2
17.22	−6.22	469.0	146.2	1088.9	2.1	6.0	0.3	28.4	6.0	52.2	0.9	2.9	0.1
17.83	−6.27	469.1	158.5	1199.0	2.6	5.7	0.5	28.7	6.5	57.3	1.0	3.3	0.2
18.81	−5.99	464.8	126.2	1441.9	2.2	6.4	0.3	28.8	5.3	67.7	0.9	3.2	0.1
19.40	−5.85	430.4	91.0	836.2	2.3	5.8	0.4	27.0	4.0	42.6	1.0	2.5	0.2
19.99	−5.70	434.4	103.5	1087.7	2.5	8.0	0.3	27.6	4.5	53.5	1.0	3.6	0.2
20.76	−5.24	451.9	161.2	1225.6	2.0	6.2	0.5	29.7	6.5	58.7	0.9	3.3	0.2
21.43	−4.89	359.7	75.0	812.0	2.1	5.8	0.2	24.0	3.3	40.7	0.8	2.4	0.1
22.68	−4.20	450.1	83.3	982.8	3.6	7.0	0.4	50.6	22.3	206.9	1.4	5.4	0.3
23.17	−4.06	478.3	164.3	911.7	4.6	8.8	0.3	32.7	6.7	45.5	0.9	3.4	0.1
23.73	−3.51	450.8	113.0	656.3	4.5	4.8	0.2	31.2	4.8	34.4	0.9	2.4	0.1
24.11	−3.19	589.8	286.7	945.3	3.8	16.6	0.7	41.3	11.3	47.5	0.9	5.1	0.2
24.78	−2.73	450.2	150.3	781.4	5.1	5.7	0.4	31.9	6.2	40.6	1.0	2.9	0.2
25.25	−2.30	475.5	239.9	1852.8	18.7	8.7	0.8	48.5	28.5	89.2	1.8	7.6	0.3
25.74	−2.16	473.5	185.0	1608.4	7.0	9.3	0.8	34.4	7.6	78.5	1.0	3.6	0.2
26.22	−1.92	545.2	417.2	2655.2	32.0	6.6	1.3	40.2	16.4	126.6	2.8	3.3	0.3
27.06	−1.16	550.4	280.0	3716.6	75.4	9.7	1.4	41.6	11.3	177.1	6.2	3.9	0.3
27.36	−1.03	466.4	390.7	2614.3	71.1	9.8	1.9	35.7	15.5	126.8	5.9	4.0	0.4

Appendix A (*continued*)

Coordinate		Concentration (ppm)						Standard deviation (1σ)					
X	Y	Sr	Na	Mg	Mn	B	Ba	Sr	Na	Mg	Mn	B	Ba
Independatrypa Lemma-2													
0.00	0.00	426.9	108.4	312.4	3.7	6.3	0.3	17.9	6.2	24.9	1.3	2.6	0.1
0.70	− 0.08	427.8	172.1	418.8	3.7	10.9	0.4	18.0	9.6	32.8	1.3	3.6	0.1
1.41	− 0.46	450.2	158.4	575.8	4.2	7.2	0.6	19.1	8.9	44.5	1.3	3.1	0.2
2.01	− 0.44	447.7	128.4	396.3	4.0	6.7	0.2	19.1	7.4	31.7	1.3	3.0	0.1
2.52	− 0.72	557.9	341.5	2038.5	9.9	11.4	0.8	23.9	19.0	154.0	1.5	3.8	0.2
3.34	− 1.20	585.7	636.2	413.6	8.9	11.3	0.8	25.2	35.3	33.5	1.5	3.9	0.2
4.05	− 1.68	545.7	289.7	404.8	5.7	9.3	0.8	23.6	16.4	32.8	1.3	3.3	0.2
4.77	− 2.15	410.3	232.0	468.7	16.4	11.8	0.5	18.2	13.6	39.3	1.7	4.0	0.2
5.38	− 2.64	434.6	115.4	392.2	4.1	6.8	0.4	19.3	7.1	32.9	1.4	2.9	0.1
6.10	− 3.11	456.8	113.0	351.3	4.4	7.3	0.2	20.4	7.0	30.0	1.5	3.2	0.1
6.91	− 3.49	433.7	124.9	491.1	4.1	7.1	0.2	19.5	7.7	41.1	1.3	3.1	0.1
7.62	− 3.77	424.5	171.0	752.4	4.4	7.3	0.3	19.2	10.4	62.5	1.5	3.1	0.1
8.33	− 3.95	437.3	79.5	398.8	4.4	7.4	0.1	19.9	5.3	34.5	1.5	2.9	0.1
9.04	− 4.32	401.6	196.7	417.3	4.3	7.2	0.1	18.4	12.1	36.1	1.5	2.9	0.1
9.65	− 4.71	395.6	152.6	367.1	4.3	7.1	0.1	18.2	9.5	32.2	1.4	2.9	0.1
10.26	− 5.09	378.6	74.4	365.3	4.2	7.0	0.2	17.5	5.1	32.2	1.4	3.0	0.1
11.26	− 5.16	402.2	132.2	323.7	4.1	6.8	0.2	18.9	8.5	29.3	1.4	2.6	0.1
11.77	− 5.34	399.1	71.0	326.1	4.2	6.9	0.2	18.9	4.9	29.7	1.4	2.6	0.1
12.48	− 5.52	411.7	69.0	295.7	4.4	7.2	0.2	19.6	4.9	27.4	1.5	2.7	0.1
13.38	− 5.59	398.9	94.8	647.3	8.1	7.6	7.7	19.1	6.5	58.1	1.7	3.1	0.7
13.98	− 5.57	369.1	90.2	666.0	4.7	7.7	3.0	17.8	6.3	60.2	1.6	3.0	0.4
14.68	− 5.75	372.1	78.9	696.5	4.6	7.5	0.3	18.1	5.6	63.3	1.5	2.9	0.1
15.38	− 5.53	519.3	245.0	3891.7	11.7	7.4	0.7	25.3	16.1	346.7	1.7	3.3	0.2
15.98	− 5.61	389.4	74.7	388.0	4.1	6.7	0.3	19.1	5.3	36.4	1.3	2.8	0.1
16.68	− 5.59	424.2	123.5	412.3	4.4	7.1	0.2	21.0	8.5	38.9	1.4	3.1	0.1
17.57	− 5.26	438.7	99.6	264.1	4.3	7.2	0.2	21.8	7.0	25.7	1.4	3.2	0.1
18.46	− 4.94	415.2	150.9	398.9	4.4	7.1	0.1	20.8	10.4	38.2	1.4	2.9	0.1
19.26	− 4.91	472.3	246.3	416.8	9.1	10.2	1.0	23.7	16.8	40.3	1.7	3.9	0.2
20.14	− 4.18	523.8	951.0	643.3	16.6	10.7	1.7	26.8	65.2	62.6	2.0	4.1	0.3
21.03	− 3.76	393.8	59.3	256.8	4.8	7.7	0.1	20.3	4.7	26.2	1.6	3.2	0.1
21.82	− 3.43	402.7	65.8	401.1	4.8	7.7	0.1	20.9	5.1	40.1	1.6	3.1	0.1
22.31	− 3.22	403.4	67.9	356.8	4.7	11.4	0.2	21.0	5.3	36.1	1.5	4.0	0.1
23.10	− 2.99	404.4	60.3	293.1	4.8	7.7	0.1	21.2	4.8	30.2	1.6	3.3	0.1
24.08	− 2.16	411.8	73.5	253.2	4.8	25.5	0.1	21.7	5.7	26.5	1.6	6.8	0.1
24.57	− 1.75	382.5	65.4	398.1	5.0	8.0	0.0	20.3	5.3	41.0	1.6	3.1	0.0
25.36	− 1.42	370.7	66.7	375.3	5.2	8.3	0.1	19.8	5.4	39.0	1.7	3.3	0.1
25.74	− 1.01	408.1	77.3	325.7	5.2	8.4	0.2	21.9	6.2	34.3	1.7	3.5	0.1
26.64	− 0.88	405.9	69.5	311.0	5.2	8.4	0.0	21.9	5.7	33.1	1.7	3.3	0.0
27.12	− 0.37	367.2	68.0	380.2	5.6	8.9	0.2	20.0	5.7	40.4	1.8	3.4	0.1
27.71	− 0.05	417.2	139.3	1275.6	5.6	9.0	0.1	22.8	10.7	132.2	1.8	3.7	0.1
28.51	0.08	399.9	124.0	1506.0	5.5	8.9	0.4	22.0	9.7	156.8	1.8	3.5	0.1

References

Azmy, K., Veizer, J., Bassett, M.G., Copper, P., 1998. Oxygen and carbon isotopic composition of Silurian brachiopods: Implications for coeval seawater and glaciations. Geol. Soc. Amer. Bull. 110, 1499–1512.

Azmy, K., Veizer, J., Wenzel, B., Bassett, M., Copper, P., 1999. Silurian strontium isotope stratigraphy. Geol. Soc. Amer. Bull. 111, 475–483.

Banner, J.L., Kaufman, J., 1994. The isotopic record of ocean chemistry and diagenesis preserved in non-luminescent brachiopods from Mississippian carbonate rocks, Illinois and Missouri. Geol. Soc. Amer. Bull. 106, 1074–1082.

Bates, N.R., Brand, U., 1991. Environmental and physiological influences on isotopic and elemental compositions of brachiopod shell calcite: implications for the isotopic evolution of Paleozoic oceans. Chem. Geol. 94, 67–78.

Bickert, T., Patzold, J., Samtleben, C., Munnecke, A., 1997. Paleoenvironmental changes in the Silurian indicated by stable isotopes in brachiopod shells from Gotland, Sweden. Geochim. Cosmochim. Acta 61, 2717–2730.

Brand, U., 1989a. Global climatic changes during the Devonian–Mississippian: stable isotope biogeochemistry of brachiopods. Palaeogeogr. Palaeoclimatol. Palaeoecol. 75, 311–329 (Global and Planetary Change Section).

Brand, U., 1989b. Aragonite-calcite transformation based on Pennsylvanian molluses. Geol. Soc. Amer. Bull. 101, 377–390.

Brand, U., 1989c. Biogeochemistry of late paleozoic North American brachiopods and secular variation of seawater composition. Biogeochemistry 7, 159–193.

Brand, U., Veizer, J., 1980. Chemical diagenesis of a multicomponent carbonate system: I. Trace elements. J. Sediment. Petrol. 50, 1219–1236.

Brand, U., Logan, A., Hiller, N., Richardson, J., 2003. Geochemistry of modern brachiopods: applications and implications for oceanography and paleoceanography. Chem. Geol. 198, 305–334.

Bruckschen, P., Veizer, J., 1997. Oxygen and carbon isotopic composition of dinantian brachiopods: paleoenvironmental implications for the lower carboniferous of Western Europe. Palaeogeogr. Palaeoclimatol. Palaeoecol. 132, 243–264.

Buening, N., Carlson, S.J., 1992. Geochemical investigation of growth in selected Recent articulate brachiopods. Lethaia 25, 331–345.

Buening, N., Spero, H.J., 1996. Oxygen- and carbon–isotope analyses of the articulate brachiopod Laqueus Californianus: a recorder of environmental changes in the subeuphotic zone. Mar. Biol. 127, 105–114.

Burke, W.H., Denison, R.E., Hetherington, E.A., Koepinck, R.B., Nelson, H.F., Otto, J.B., 1982. Variation of seawater $^{87}Sr/^{86}Sr$ throughout Phanerozoic time. Geology 10, 516–519.

Carpenter, S.J., Lohmann, K.C., 1995. $\delta^{18}O$ and $\delta^{13}C$ values of modern brachiopod shells. Geochim. Cosmochim. Acta 59, 3749–3764.

Chen, Y., Wang, H., 1996. The comprehensive stratigraphic from work of Devonian in Longmenshan area, Sichuan, China. In: Liu, W., Chen, Y., et al. (Eds.), Sequence stratigraphy, Devonian in Longmenshan area: II. Press of Chengdu Univ. Sci. and Tech., Chengdu, pp. 12–29.

Diener, A., Ebneth, S., Veizer, J., Buhl, D., 1996. Strontium isotope stratigraphy of the Middle Devonian: brachiopod and conodonts. Geochim. Cosmochim. Acta 60, 639–652.

Dodd, J.R., 1967. Magnesium and strontium in calcareous skeletons: a review. J. Paleontol. 41, 1313–1329.

Gao, S., Liu, X., Yuan, H., Hattendorf, B., Günther, D., Chen, L., Hu, S., 2002. Determination of forty-two major and trace elements in USGS and NIST SRM glasses by laser ablation-inductively coupled plasma-mass spectrometry. J. Geostand. and Geoanalysis 26, 181–195.

Grossman, E.L., Zhang, C., Yancey, T.E., 1991. Stable isotope stratigraphy of brachiopods from Pennsylvanian shales in Texas. Geol. Soc. Amer. Bull. 103, 953–965.

Grossman, E.L., Mii, H.S., Yancey, T.E., 1993. Stable isotopes in late Pennsylvanian brachiopods from the United States: implications for carboniferous paleogeography. Geol. Soc. Amer. Bull. 105, 1284–1296.

Grossman, E.L., Mii, H., Zhang, Ch., Yancey, T.E., 1996. Chemical variation in Pennsylvanian brachiopod shells-diagenetic, taxonomic, microstructural, and seasonal effects. J. Sed. Res. 66 (5), 1011–1022.

Gunther, D., Frischknecht, R., Heinrich, C.A., Kahlert, H.J., 1997. Capabilities of an ArF193 nm excimer laser for LAM-ICP-MS micro-analysis of geological materials. J. Anal. At. Spectrom. 12, 9393–9944.

Gunther, D., Jackson, S.E., Longerich, H.P., 1999. Laser ablation and arc/spark solid sample introduction into inductively coupled plasma-mass spectrometers. Spectrochim. Acta 54B, 381–409.

James, N.P., Bone, Y., Kyser, T.K., 1997. Brachiopod $\delta^{18}O$ values do reflect ambient oceanography: lacepede shelf, Southern Australia. Geology 25, 551–554.

Land, L.S., 1995. Comment on "Oxygen and carbon isotopic composition of Ordovician brachiopods: implications for coeval seawater" by H. Qing and J. Veizer. Geochim. Cosmochim. Acta 59, 2843–2844.

Lavoie, D., 1993. Early devonian marine isotopic signatures: brachiopods from the upper Gaspe limestones, Gaspe Peninsula, Quebec, Canada. J. Sediment. Petrol. 63, 620–627.

Lea, D.W., Pak, D.K., Spero, H.J., 2000. Climate impact of late Quaternary equatorial Pacific Sea surface temperature variations. Science 289, 1719–1724.

Lee, X., Wan, G., 2000. No vital effect on $\delta^{18}O$ and $\delta^{13}C$ values of fossil brachiopod shells: evidence from Middle Devonian in China. Geochim. Cosmochim. Acta 64, 2649–2664.

Lee, X., Wan, G., Huang, R., 1999. Different fossil brachiopod skeletal microstructure tells of different information on carbon and oxygen isotope contents. Chin. Sci. Bull. 44, 2087–2094.

Liu, W., Zheng, Y., Li, X., 1996. Reconstruction of paleogeography and paleotectonics of devonian in longmenshan area, Sichuan, China. In: Liu, W., Chen, Y., et al. (Eds.), Sequence Stratigraphy, Devonian in Longmenshan area: II. Press of Chengdu Univ. Sci. Tech., Chengdu, pp. 62–75.

Longerich, H.P., Jackson, S.E., Gunther, D., 1996. Laser ablation inductively coupled plasma mass spectrometric transient signal

data acquisition and analyte concentration calculation. J. Anal. At. Spectrom. 11, 899–904.

Lowenstam, H.A., 1961. Mineralogy, O^{18}/O^{16} ratios and strontium and magnesium contents of recent and fossil brachiopods and their bearing on the history of the oceans. J. Geol. 69, 241–260.

Mii, H., Grossman, E.L., Yancey, T.E., 1997. Stable carbon and oxygen isotope shifts in Permian Seas of West Spitsbergen—global change or diagenetic artifact? Geology 25, 227–230.

Mii, H., Grossman, E.L., Yancey, T.E., 1999. Carboniferous isotope stratigraphies of North America: implications for carboniferous paleoceanography and Mississippian glaciation. Geol. Soc. Amer. Bull. 111, 960–973.

Moberly Jr., R., 1968. Composition of magnesian calcites of algae and pelecypods by electron microprobe analysis. Sediment 11, 61–82.

Morrison, J.O., Brand, U., 1986. Geochemistry of recent marine invertebrates. Geosci. Can. 13, 237–254.

Pearce, N.J.G., Perkins, W.T., Westgate, J.A., Gorton, M.P., Jackson, S.E., Neal, C.R., Chenery, S.P., 1997. A compilation of new and published major and trace element data for NIST SRM 610 and NIST SRM 612 glass reference materials. J. Geostand. Geoanalysis 21, 115–141.

Pierson, B.J., 1981. The control of cathodoluminescence in dolomite by iron and manganese. Sediment 28, 601–610.

Popp, B.N., Anderson, T.F., Sandberg, P.A., 1986. Textural, elemental and isotopic variations among constituents in Middle Devonian limestones, North America. J. Sediment. Petrol. 56, 715–727.

Qing, H., Veizer, J., 1994. Oxygen and carbon isotopic composition of Ordovician brachiopods: implications for coeval sea water. Geochim. Cosmochim. Acta 58, 4429–4442.

Qing, H., Barnes, C.R., Buhl, D., Veizer, J., 1998. The strontium isotopic composition of Ordovician and Silurian brachiopods and conodonts: relationships to geological events and implications for coeval seawater. Geochim. Cosmochim. Acta 62, 1721–1733.

Railsback, L.B., 1990. Influence of changing deep ocean circulation on the Phanerozoic oxygen isotope record. Geochim. Cosmochim. Acta 54, 1501–1509.

Railsback, L.B., Anderson, T.F., Ackerly, S.D., Cisne, J.L., 1989. Paleoceanographic modeling of temperature-salinity profiles from stable isotopic data. Paleoceanography 4, 585–591.

Rao, C.P., 1996. Elemental composition of marine calcite from modern temperate brachiopods, bryozoans and bulk carbonates, Eastern Tasmania, Australia. Carbonates and Evaporites 11, 1–18.

Rosenberg, G.D., Hughes, W.W., 1989. Ontogenetic variations in the distribution of Ca and Mg in skeletal tissues of vertebrates and invertebrates. In: Crick, R.E. (Ed.), Origin, Evolution, and Modern Aspects of Biomineralization in Plants and Animals. Plenum Press, New York, pp. 339–347.

Rudwick, M.J.S., 1959. The growth and form of brachiopod shells. Geol. Mag. XCVI, 1–24.

Rush, P.F., Chafetz, H.S., 1990. Fabric-retentive, non-luminescent brachiopods as indicators of original $\delta^{13}C$ and $\delta^{18}O$ composition: a test. J. Sediment. Petrol. 60, 968–981.

Talent, J.A., Mawson, R., Andrew, A.S., Hamilton, P.J., Whitford, D.J., 1993. Middle palaeozoic extinction events: faunal and isotopic data. Palaeogeogr. Palaeoclimatol. Palaeoecol. 104, 139–152.

Veizer, J., 1983a. Chemical diagenesis of carbonate rocks: theory and application of trace element technique. In: Arthur, M.A., Anderson, T.F., Kaplan, I.R., et al. (Eds.), Stable Isotopes in Sedimentary Geology, p.III/1-III/100, short Course Notes, vol. 10. SEPM, Tulsa, Okla.

Veizer, J., 1983b. Trace elements and isotopes in sedimentary carbonates. Rev. Miner. 11, 265–300.

Veizer, J., 1995. Reply to the comment by L.S. Land on "Oxygen and carbon isotopic composition of ordovician brachiopods: implications for coeval seawater". Geochim. Cosmochim. Acta 59, 2845–2846.

Veizer, J., Hoefs, J., 1976. The nature of O^{18}/O^{16} and C^{13}/C^{12} secular trends in sedimentary carbonate rocks. Geochim. Cosmochim. Acta 40, 1387–1395.

Veizer, J., Fritz, P., Jones, B., 1986. Geochemistry of brachiopods: oxygen and carbon isotopic records of Paleozoic oceans. Geochim. Cosmochim. Acta 40, 1679–1696.

Veizer, J., Bruckschen, P., Pawellek, F., Diener, A., Podlaha, O.G., Carden, G.A.F., Jasper, T., Korte, C., Strauss, H., Azmy, K., Ala, D., 1997a. Oxygen isotope evolution of phanerozoic seawater. Palaeogeogr. Palaeoclimatol. Palaeoecol. 132, 159–172.

Veizer, J., Buhl, D., Diener, A., Ebneth, S., Podlaha, O.G., Bruckschen, P., Jasper, T., Korte, C., Schaaf, M., Ala, D., Azmy, K., 1997b. Strontium isotope stratigraphy:potential resolution and event correlation. Palaeogeogr. Palaeoclimatol Palaeoecol. 132, 65–77.

Wadleigh, M.A., Veizer, J., 1992. $^{18}O/^{16}O$ and $^{13}C/^{12}C$ in lower Paleozoic articulate brachiopods: implication for the isotopic composition of seawater. Geochim. Cosmochim. Acta 56, 431–443.

Wenzel, B., Joachimski, M.M., 1996. Carbon and oxygen isotopic composition of Silurian brachiopods (Gotland/Sweden): palaeoceanograhic implications. Palaeogeogr. Palaeoclimatol. Palaeoecol. 122, 143–166.

Williams, A., 1966. Growth and structure of the shell of living articulate brachiopods. Nature 10, 1146–1148.

Williams, A., 1968. Evolution of the shell structure of articulate brachiopods. Spec. Pap. Palaeontol. 2, 1–55.

Zachos, J.C., Lohmann, K.C., Walker, J.C.G., Wise, S.W., 1993. Abrupt climate change and transient climates during the Paleogene: a marine perspective. J. Geol. 101, 191–213.